Journal of Computational Physics 229 (2010) 4869–4883

Contents lists available at ScienceDirect

Journal of Computational Physics

journal homepage: www.elsevier.com/locate/jcp

Bloch decomposition-based Gaussian beam method for the Schrödinger equation with periodic potentials

Shi Jin [a,*], Hao Wu [b], Xu Yang [a,1], Zhongyi Huang [b]

[a] Department of Mathematics, University of Wisconsin, Madison, WI 53706, USA
[b] Department of Mathematical Sciences, Tsinghua University, Beijing 10084, China

ARTICLE INFO

Article history:
Received 5 January 2009
Received in revised form 18 January 2010
Accepted 19 January 2010
Available online 28 January 2010

Keywords:
Schrödinger equation
Periodic potential
Bloch decomposition
Gaussian beam method
Liouville equation

ABSTRACT

The linear Schrödinger equation with periodic potentials is an important model in solid state physics. The most efficient direct simulation using a Bloch decomposition-based time-splitting spectral method [18] requires the mesh size to be $O(\epsilon)$ where ϵ is the scaled semiclassical parameter. In this paper, we generalize the Gaussian beam method introduced in Jin et al. [23] to solve this problem asymptotically. We combine the technique of Bloch decomposition and the Eulerian Gaussian beam method to arrive at an Eulerian computational method that requires mesh size of $O(\sqrt{\epsilon})$. The accuracy of this method is demonstrated via several numerical examples.

1. Introduction

The linear Schrödinger equation with periodic potentials

$$i\epsilon\frac{\partial \Psi^\epsilon}{\partial t} = -\frac{\epsilon^2}{2}\Delta\Psi^\epsilon + V_\Gamma\left(\frac{\boldsymbol{x}}{\epsilon}\right)\Psi^\epsilon + U(\boldsymbol{x})\Psi^\epsilon, \quad \boldsymbol{x}\in\mathbb{R}^n, \tag{1.1}$$

is a simple model in solid state physics which describes the motion of electrons with the periodic potentials generated by the ionic cores. Here $\Psi^\epsilon(t,\boldsymbol{x})$ is the wave function, ϵ is the re-scaled Plank constant in the semiclassical regime, and $U(\boldsymbol{x})$ is the smooth external potential. The oscillatory *lattice-potential* $V_\Gamma(\boldsymbol{z})$ is a periodic function in some *regular lattice* Γ.

We consider this model in *one dimension* with the *two-scale* WKB initial condition:

$$\Psi_0^\epsilon\left(x, z := \frac{x}{\epsilon}\right) = A_0(x,z)e^{iS_0(x)/\epsilon}. \tag{1.2}$$

Without loss of generality we assume $\Gamma = 2\pi\mathbb{Z}$, i.e.

$$V_\Gamma(z+2\pi) = V_\Gamma(z), \quad \forall z\in\mathbb{R}. \tag{1.3}$$

We introduce several physical concepts related to (1.3) [1]:

* Corresponding author. Tel.: +1 608 263 3302; fax: +1 608 263 8891.
E-mail addresses: jin@math.wisc.edu (S. Jin), hwu@tsinghua.edu.cn (H. Wu), xuyang@math.princeton.edu (X. Yang), zhuang@math.tsinghua.edu.cn (Z. Huang).
[1] Present address: Program in Applied and Computational Mathematics, Princeton University, Princeton, NJ 08544, USA.

0021-9991/$ - see front matter © 2010 Elsevier Inc. All rights reserved.
doi:10.1016/j.jcp.2010.01.025

- The fundamental domain of the lattice Γ is $\mathcal{C} = (0, 2\pi)$.
- The dual lattice $\Gamma^* = \mathbb{Z}$.
- The (first) Brillouin zone is $\mathcal{B} = (-\frac{1}{2}, \frac{1}{2})$, which is the fundamental domain of Γ^*.

The direct numerical simulation of (1.1) and (1.2) is prohibitively expensive due to the small parameter ϵ in the semiclassical regime and the highly oscillating structure of V_Γ. The standard time-splitting spectral method [3] requires the mesh size be $o(\epsilon)$ and the time step be $o(\epsilon)$. A novel time-splitting spectral method based on the Bloch decomposition was proposed recently by Huang et al. [18–20] which relaxes the time step requirement to be $O(1)$ with a much coarser mesh size of $O(\epsilon)$. However, such a mesh size is still expensive especially in high dimensions for a very small ϵ.

One efficient alternative way is to solve (1.1) and (1.2) asymptotically by the Bloch band decomposition and the modified WKB method [4], which leads to eikonal and transport equations in the semiclassical regime. The problem of these approaches is that they do not give accurate solution around caustics. The Gaussian beam method, developed for the high frequency linear waves [34,38,37,29,30,23], and also in the setting of quantum mechanics [14–16], provides an efficient way to compute the wave amplitude around caustics. The idea is to allow the phase function to be *complex* and choose the imaginary part properly so that the solution has a Gaussian profile. The detailed construction and its validity at caustics were analyzed by Ralston etc. in [35,7]. All these previous works gave the Gaussian beam method in the Lagrangian framework.

In [23], we developed an Eulerian Gaussian beam method to solve the linear Schrödinger equation asymptotically. The method consists of solving n complex-valued and 1 real-valued homogeneous Liouville equations for n-space dimensional problems. The solution to this method has been showed to have good accuracy even at caustics, with a mesh size as coarse as $O(\sqrt{\epsilon})$. There have also been other Eulerian Gaussian beam methods [26] that use much more complex-valued inhomogeneous Liouville equations. In this paper, we generalize our method in [23] for (1.1), (1.2) with the help of the Bloch decomposition. The idea is to use the Eulerian Gaussian beam method of [23] for each of the Bloch band, and then superimpose them for all the bands. (This method is restricted to adiabatic cases which do not permit band-crossings.) Since effectively only small number of bands are needed numerically and the Liouville equation is solved locally in the vicinity of a co-dimensional zero level curve [31,33,28], the overall cost of this method is much smaller than a full simulation by directly solving (1.1) when ϵ is small.

For periodic potentials, every energy band could yield caustics in the semiclassical regime. Since the solution is a superposition of many energy bands, there could be many caustics thus significantly reduce the overall accuracy of the semiclassical method. Thus methods accurate near caustics are highly desirable for such problems.

The paper is organized as follows. In Section 2 we give an overview of the Bloch decomposition and the semiclassical limit of the Schrödinger equation with periodic structures. In Section 3, we formulate the Gaussian beam method for solving (1.1) and (1.2) by combining the Bloch decomposition with the Eulerian Gaussian beam method of [23]. We show the accuracy and efficiency of this Gaussian beam method through several numerical examples in Section 4. In Section 4.3, we study an insulator example. Finally, we make some conclusive remarks in Section 5.

2. Overview of the Bloch decomposition and the semiclassical limit

2.1. The Bloch decomposition

Define $E_m(k)$ as the mth eigenvalue and $\chi_m(k,z)$ as the corresponding mth eigenfunction of the shifted Hamiltonian $H(k,z)$:

$$H(k,z) := \frac{1}{2}(-i\partial_z + k)^2 + V_\Gamma(z), \tag{2.1}$$

$$H(k,z)\chi_m(k,z) = E_m(k)\chi_m(k,z), \tag{2.2}$$

$$\chi_m(k,z+2\pi) = \chi_m(k,z), \quad z \in \mathbb{R}, \quad k \in \mathcal{B}. \tag{2.3}$$

$E_m(k)$, $k \in \mathcal{B}$, is called the mth energy band, and $\{E_m(k), \chi_m(k,z)\}_m$ describe the spectral properties of the shifted Hamiltonian $H(k,z)$. It has been shown in [40] that there exists an ordered countable family of real eigenvalues $\{E_m(k)\}_{m=1}^\infty$ such that

$$E_1(k) \leqslant E_2(k) \leqslant \cdots \leqslant E_m(k) \leqslant \cdots, \quad m \in \mathbb{N},$$

and the complete set of the eigenfunctions $\{\chi_m(k,z)\}_{m=1}^\infty$ for each $k \in \mathcal{B}$ forms an orthonormal basis of $L^2(\mathcal{C})$. This allows for a decomposition of the initial condition (1.2) in terms of Bloch waves with the help of the stationary phase method (cf. [4, Sections 3.2 and 4.7 of Chapter 4]):

$$\Psi_0^\epsilon(x,z) = \sum_{m=1}^\infty a_m^0(x)\chi_m(\partial_x S_0, z)e^{iS_0(x)/\epsilon} + O(\epsilon), \tag{2.4}$$

where the coefficient

$$a_m^0(x) = \int_0^{2\pi} A_0(x,z)\overline{\chi}_m(\partial_x S_0, z)\mathrm{d}z. \tag{2.5}$$

2.2. The semiclassical limit and its computation

Plugging the modified WKB ansatz:

$$\Psi^\epsilon(t,x) = A\Big(t,x,\frac{x}{\epsilon}\Big)e^{iS(t,x)/\epsilon}, \tag{2.6}$$

into (1.1) yields, to the leading order, the following eikonal equation for S_m and transport equation for a_m via a separation of the slow scale x and fast scale x/ϵ (cf. [4]):

$$\partial_t S_m + E_m(\partial_x S_m) + U(x) = 0, \tag{2.7}$$

$$\partial_t a_m + E_m'(\partial_x S_m)\partial_x a_m + \frac{1}{2}a_m\partial_x\big(E_m'(\partial_x S_m)\big) + \beta_m a_m = 0, \tag{2.8}$$

where $\beta_m(t,x) \in i\mathbb{R}$ is given by

$$\beta_m = \langle\partial_t\chi_m,\chi_m\rangle_{L^2(\mathcal{C})} - \frac{1}{2}\partial_x\big(E_m'(\partial_x S_m)\big) - \frac{i}{2}\langle(\partial_z + i\partial_x S_m)\partial_x\chi_m + \partial_x(\partial_z + i\partial_x S_m)\chi_m,\chi_m\rangle_{L^2(\mathcal{C})} \tag{2.9}$$

with χ_m evaluated at $k = \partial_m S_m(t,x)$ and $\langle\cdot,\cdot\rangle_{L^2(\mathcal{C})}$ defined as

$$\langle f,g\rangle_{L^2(\mathcal{C})} = \int_0^{2\pi} f\bar{g}\mathrm{d}z.$$

The solution to (1.1) is approximated by

$$\Psi^\epsilon(t,x) = \sum_{m=1}^{\infty} a_m(t,x)\chi_m\Big(\partial_x S_m,\frac{x}{\epsilon}\Big)e^{iS_m(t,x)/\epsilon} + O(\epsilon). \tag{2.10}$$

Note that since $\beta_m(t,x) \in i\mathbb{R}$, the following conservation law holds [4]:

$$\partial_t|a_m|^2 + \partial_x(E_m'(\partial_x S_m)|a_m|^2) = 0.$$

The solution to the Hamilton–Jacobi Eq. (2.7) develops singularities when caustic forms, and the correct semiclassical limit of the physical observables (density, velocity, etc.), as $\epsilon \to 0$, becomes multivalued beyond caustics. To describe the dynamics beyond caustics, one can use the Wigner transform to obtain the Liouville equation along each band [2]:

$$\mathcal{L}_m w_m = \partial_t w_m + E_m'(\xi)\partial_y w_m - U\prime(y)\partial_\xi w_m = 0, \tag{2.11}$$

where $w_m(t,x,\xi) > 0$ is the density distribution of the mth energy band of the particle. The operator $\mathcal{L}_m$ is the linear Liouville operator for the mth energy band. The semiclassical limit initial data for w_m, for (1.2), is measure-valued:

$$w_m(0,x,\xi) = |a_m^0|^2\delta(\xi - \partial_x S_0), \tag{2.12}$$

where a_m^0 is given by (2.5).

The (multivalued) physical observables such as $\rho_m, u_m = \partial_x S_m$ etc. can be evaluated by taking the moments of w_m over ξ.

An efficient numerical method to solve the Liouville Eq. (2.11) with initial data (2.12) was introduced in [6,21,22], through a decomposition of $w_m = f_m\delta(\phi_m)$ where both f_m and ϕ_m solve the same Liouville equation for the mth energy band (in the level set framework):

$$\mathcal{L}_m\phi_m = 0, \quad \mathcal{L}_m f_m = 0.$$

One can compute the multivalued densities by

$$\rho_m(t,y) \in \left\{\frac{f(t,y,\xi)}{|\partial_\xi\phi_m|}\middle|\phi_m(t,y,\xi) = 0\right\}. \tag{2.13}$$

Based on this formulation, a level set method for the semiclassical limit of (1.2) was introduced in [27]. For the computations of multivalued solutions to this problem see also [10–13]. The problems with all these semiclassical methods is that ρ_m defined in (2.13) blows up at caustics since $\partial_\xi\phi_m = 0$.

In Section 3, we will introduce the Bloch decomposition-based Gaussian beam method to solve (1.1) and (1.2), which is a generalization of the Eulerian Gaussian beam method we developed in [23]. The key difference from (2.13) is that, one can get rid of the singularities of $|\partial_\xi\phi_m|$ by *making* ϕ_m *complex*.

2.3. Numerical computation of the Bloch bands

In this subsection, we briefly restate the numerical computation of the Bloch bands $\{E_m(k),\chi_m(k,z)\}_m$ for convenience. The details are referred to [18, Section 2.2].

Define the Fourier transform of χ_m as

$$\widehat{\chi}_m(k,\lambda) = \frac{1}{2\pi}\int_0^{2\pi}\chi_m(k,z)e^{-i\lambda z}\mathrm{d}z.$$

By taking the Fourier transform of (2.2), one has

$$\frac{(\lambda+k)^2}{2}\widehat{\chi}_m(k,\lambda)+\frac{1}{2\pi}\int_0^{2\pi} e^{-i\lambda z}V_\Gamma(z)\chi_m(k,z)\mathrm{d}z = E_m(k)\widehat{\chi}_m(k,\lambda). \tag{2.14}$$

The discrete formula of (2.14) for $\lambda\in\{-\Lambda,\dots,\Lambda-1\}\subset\mathbb{Z}$ reads as

$$\mathbf{H}(k,\Lambda)\begin{pmatrix}\widehat{\chi}_m(k,-\Lambda)\\ \widehat{\chi}_m(k,1-\Lambda)\\ \vdots\\ \widehat{\chi}_m(k,\Lambda-1)\end{pmatrix} = E_m(k)\begin{pmatrix}\widehat{\chi}_m(k,-\Lambda)\\ \widehat{\chi}_m(k,1-\Lambda)\\ \vdots\\ \widehat{\chi}_m(k,\Lambda-1)\end{pmatrix}, \tag{2.15}$$

where the $2\Lambda\times 2\Lambda$ matrix $\mathbf{H}(k,\Lambda)$ is given by

$$\mathbf{H}(k,\Lambda)=\begin{pmatrix}\frac{(-\Lambda+k)^2}{2}+\widehat{V}_\Gamma(0) & \widehat{V}_\Gamma(-1) & \cdots & \widehat{V}_\Gamma(1-2\Lambda)\\ \widehat{V}_\Gamma(1) & \frac{(-\Lambda+1+k)^2}{2}+\widehat{V}_\Gamma(0) & \cdots & \widehat{V}_\Gamma(2-2\Lambda)\\ \vdots & \vdots & \ddots & \vdots\\ \widehat{V}_\Gamma(2\Lambda-1) & \widehat{V}_\Gamma(2\Lambda-2) & \cdots & \frac{(\Lambda-1+k)^2}{2}+\widehat{V}_\Gamma(0)\end{pmatrix}.$$

The eigenfunction $\chi_m(k,z)$ is computed by

$$\chi_m(k,z)=\int_{-\infty}^{+\infty}\widehat{\chi}_m(k,\lambda)e^{i\lambda z}\mathrm{d}\lambda\approx\sum_{\lambda=-\Lambda}^{\Lambda-1}\widehat{\chi}_m(k,\lambda)e^{i\lambda z}.$$

3. A Bloch decomposition-based Gaussian beam method

In this section we give the Bloch decomposition-based Gaussian beam method using both the Lagrangian and Eulerian formulations. We first briefly introduce the Lagrangian formulation for solving the Schrödinger equation with periodic potentials, then focus on the Eulerian formulation.

3.1. The Lagrangian formulation

In this subsection, we adopt the Gaussian beam approximation to the mth energy band of the Schrödinger Eq. (1.1). Denote

$$\varphi_{la}^{\epsilon,m}(t,x,y_0)=a_m(t,y_m)\tilde{\chi}_m\Big(\partial_x T_m,\frac{x}{\epsilon}\Big)e^{iT_m(t,x,y_m)/\epsilon}, \tag{3.1}$$

where $y_m=y_m(t,y_0)$, and $T_m(t,x,y_m)$ is a second order Taylor truncated phase function

$$T_m(t,x,y_m)=S_m(t,y_m)+p_m(t,y_m)(x-y_m)+\frac{1}{2}M_m(t,y_m)(x-y_m)^2.$$

Note that $S_m\in\mathbb{R}, p_m\in\mathbb{R}, a_m\in\mathbb{C}, M_m\in\mathbb{C}$. $\tilde{\chi}_m\big(\partial_x T_m,\frac{x}{\epsilon}\big)$ is $\chi_m\big(k,\frac{x}{\epsilon}\big)$ with *real*-valued k replaced by *complex*-valued $\partial_x T_m$ and

$$\tilde{\chi}_m(k,z)=\chi_m(k,z)\quad\text{for}\quad k\in\mathbb{R}.$$

Using the Lagrangian beam summation formula (for example [17]) and (2.10), one has the Lagrangian Gaussian beam solution to (1.1) as

$$\Phi_{la}^{\epsilon}(t,x)=\sum_{m=1}^{\infty}\int_{\mathbb{R}}\frac{1}{\sqrt{2\pi\epsilon}}r_\theta(x-y_m(t,y_0))\varphi_{la}^{\epsilon,m}(t,x,y_0)\mathrm{d}y_0, \tag{3.2}$$

in which $r_\theta\in C_0^\infty(\mathbb{R}^n), r_\theta\geqslant 0$ is a truncation function with $r_\theta\equiv 1$ in a ball of radius $\theta>0$ about the origin and the trajectory of the beam center y_m is chosen as

$$\frac{\mathrm{d}y_m}{\mathrm{d}t}=E_m'(p_m),\quad y_m(0)=y_0.$$

By a similar derivation of the Lagrangian formulation as in [23, Section 2.1], one has the set of the evolutionary ODEs (the details of the derivation are given in Appendix A):

$$\frac{dy_m}{dt} = E_m'(p_m), \tag{3.3}$$

$$\frac{dp_m}{dt} = -U'(y_m), \tag{3.4}$$

$$\frac{dM_m}{dt} = -E_m''(p_m)M_m^2 - U''(y_m), \tag{3.5}$$

$$\frac{dS_m}{dt} = E_m'(p_m)p_m - E_m(p_m) - U(y_m), \tag{3.6}$$

$$\frac{da_m}{dt} = -\frac{1}{2}E_m''M_m a_m + u_{m,1}(p_m)U'(y_m)a_m, \tag{3.7}$$

where $u_{m,1}$ is given by

$$u_{m,1}(k) = \langle \partial_k \chi_m, \chi_m \rangle_{L^2(C)}, \tag{3.8}$$

and $y_m = y_m(t,y_0)$, $p_m = p_m(t,y_m(t,y_0))$, $M_m = M_m(t,y_m(t,y_0))$, $S_m = S_m(t,y_m(t,y_0))$, $a_m = a_m(t,y_m(t,y_0))$. Note that $u_{m,1} \in i\mathbb{R}$, and $u_{m,1}U'(y_m)$ is the so-called Berry-phase in [5,32,36], which is importantly related to the Quantum Hall effects in physics [36].

The Eqs. (3.3) and (3.4) are called the ray tracing equations; (3.5) is a Riccati equation for the Hessian M_m, which could be solved by the dynamic first order system of ray tracing equations:

$$\frac{dP_m}{dt} = E_m''(p_m)R_m, \quad \frac{dR_m}{dt} = -U''(y_m)P_m, \tag{3.9}$$

$$M_m(t,y_m(t,y_0)) = R_m P_m^{-1}. \tag{3.10}$$

According to [37,23] we specify the initial conditions for (3.3)–(3.7) as

$$y_m(0,y_0) = y_0, \tag{3.11}$$

$$p_m(0,y_0) = \partial_y S_0(y_0), \tag{3.12}$$

$$M_m(0,\boldsymbol{y}_0) = \partial_y^2 S_0(y_0) + i, \tag{3.13}$$

$$S_m(0,y_0) = S_0(y_0), \tag{3.14}$$

$$a_m(0,y_0) = a_m^0(y_0), \tag{3.15}$$

where a_m^0 is given by (2.5).

When one computes the Lagrangian beam summation integral using (3.1) and (3.2), the *complex*-valued $\partial_x T_m = p_m + (x-y_m)M_m$ could be approximated by the *real*-valued p_m with the Taylor truncated error of $O(|x-y_m|)$, i.e.

$$\Phi_{la}^{\epsilon}(t,x) = \sum_{m=1}^{\infty} \int_{\mathbb{R}} \frac{1}{\sqrt{2\pi\epsilon}} r_\theta(x-y_m)a_m(t,y_m)\tilde{\chi}_m\left(p_m, \frac{x}{\epsilon}\right) e^{iT_m(t,x,y_m)/\epsilon} dy_0 + O(|x-y_m|). \tag{3.16}$$

Since $|x-y_m|$ is of $O(\sqrt{\epsilon})$ (cf. [37,23]), this approximation does not destroy the total accuracy of the Gaussian beam method, yet it provides the benefit that the eigenfunction $\tilde{\chi}_m(k,z)$ is only evaluated for real-valued k which implies $\tilde{\chi}_m(k,z) = \chi_m(k,z)$.

3.2. The Eulerian formulation

In this subsection, by an application of a similar technique developed in [23] we introduce the Eulerian Gaussian beam formulation using the level set method to solve (1.1), (1.2).

First, corresponding to ray tracing Eqs. (3.3) and (3.4), an Eulerian level set method for computing (multivalued) velocity $u_m = \partial_x S_m$ solves for the zero level set of ϕ_m which satisfies the homogeneous Liouville equation [6,22]:

$$\mathcal{L}_m \phi_m = 0, \tag{3.17}$$

where $\mathcal{L}_m$ is defined in (2.11). Next, since the Lagrangian system (3.6) and (3.7) is defined on the rays (characteristics), its Eulerian formulation can be written as [26]:

$$\mathcal{L}_m S_m = E_m'(\xi)\xi - E_m(\xi) - U(y), \tag{3.18}$$

$$\mathcal{L}_m a_m = -\frac{1}{2}E_m''(\xi)M_m a_m + u_{m,1}(\xi)U'(y)a_m, \tag{3.19}$$

and $u_{m,1}$ is determined by (3.8). It was observed in [23] that, *if* ϕ_m *is complex*, then M_m in (3.19) can be obtained from

$$M_m = -\frac{\partial_y \phi_m}{\partial_\xi \phi_m}.$$

To be compatible with the initial data (3.13)–(3.15), we use the following initial conditions:

$$\phi_m(0,y,\xi) = -iy + (\xi - \partial_y S_0) \tag{3.20}$$

$$S_m(0,y,\xi) = S_0(y), \quad a_m(0,y,\xi) = a_m^0(y), \tag{3.21}$$

where a_m^0 is given by (2.5).

By essentially identical proofs as in [23, Theorem 3.2], one could see that (3.21) *complexifies* the Liouville Eq. (3.17) and makes $\partial_\xi \phi_m$ *non-degenerate* for all $t > 0$.

The multivalued velocity u_m is given by the zero level set of the *real* part of ϕ_m, i.e.

$$\text{Re}\ \phi_m(t,y,u_m) = 0$$

Define

$$\varphi_{eu}^{\epsilon,m}(t,x,y,\xi) = a_m(t,y,\xi)\chi_m\left(\xi,\frac{x}{\epsilon}\right)e^{iT_m(t,x,y,\xi)/\epsilon}, \tag{3.22}$$

where

$$T_m(t,x,y,\xi) = S_m(t,y,\xi) + \xi(x-y) + \frac{1}{2}M_m(t,y,\xi)(x-y)^2,$$

then the Eulerian beam summation formula corresponding to (3.16) is given by (cf. [23])

$$\Phi_{eu}^{\epsilon}(t,x) = \sum_{m=1}^{\infty}\int_{\mathbb{R}}\int_{\mathbb{R}}\frac{1}{\sqrt{2\pi\epsilon}}r_0(x-y)\varphi_{eu}^{\epsilon,m}(t,x,y,\xi)\delta(\text{Re}[\phi_m])\mathrm{d}\xi\mathrm{d}y. \tag{3.23}$$

Remark 3.1. Eq. (3.23) could be solved by a discretized delta function integral method [39] or a local semi-Lagrangian method introduced in [23, Section 3.3] which is an improved version of the semi-Lagrangian method designed in [26].

Remark 3.2. The curve integration method for the computation of phase S from a given multivalued velocity $u = \partial_x S$ introduced in [9,24] cannot be used here since the integration constant, which cannot be ignored when evaluating (3.23), is different for different bands. Therefore we use the inhomogeneous Liouville Eq. (3.18) to compute the phase function directly, as in [26].

Remark 3.3. Although the Liouville equations are defined in the phase-space, thus the computational dimension is doubled than a direct computation of the Schrödinger Eq. (1.1), one only needs to solve the Liouville equations *locally* in the vicinity of a co-dimensional zero level curve of $\text{Re}(\phi_m)$ [31,33,28], hence with a mesh size of $O(\sqrt{\epsilon})$, the overall cost of this method is much smaller than a full simulation by directly solving (1.1) when ϵ is small. For cost analysis of the Eulerian Gaussian beam method see [23].

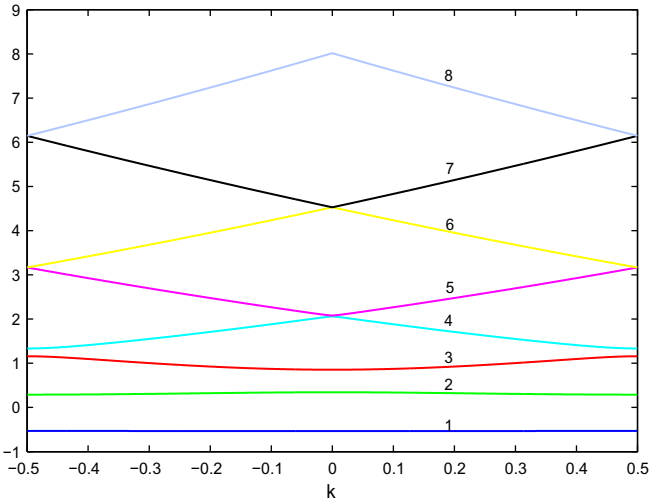

Fig. 1. The eigenvalues $E_m(k)$, $m = 1,\ldots,8$ of the Mathieu's model.

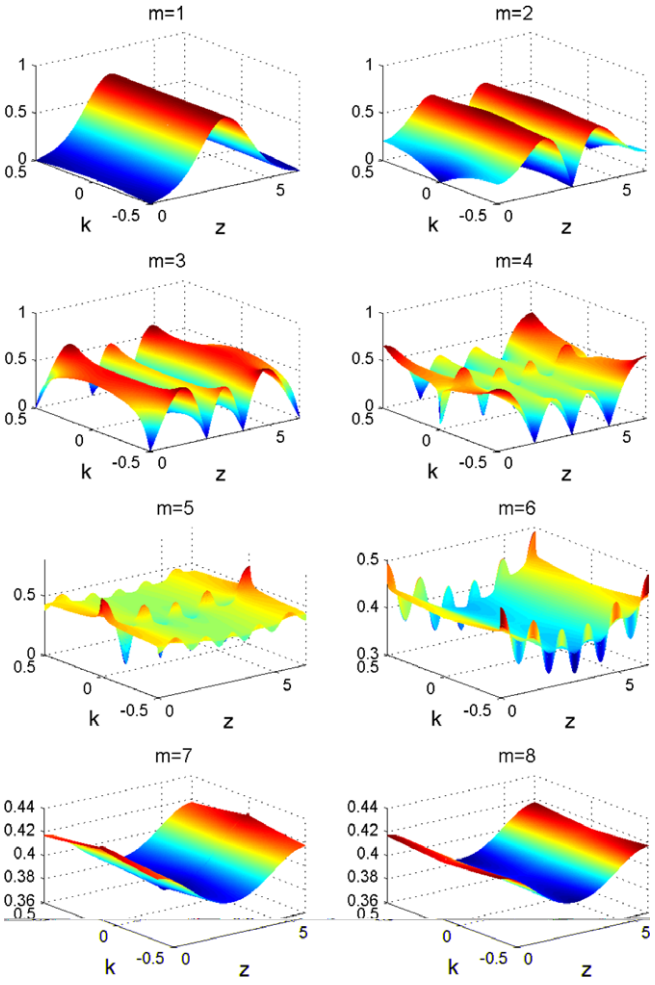

Fig. 2. The modulus of the eigenfunctions $|\chi_m(k,z)|^2$, $m = 1,\ldots,8$ of the Mathieu's model.

Table 1
The l^2 errors of Bloch decomposition for the initial data (4.1).

M	6	8	10	12
$\epsilon = 1/128$	5.49×10^{-4}	9.85×10^{-6}	1.10×10^{-7}	8.37×10^{-10}
$\epsilon = 1/512$	5.49×10^{-4}	9.85×10^{-6}	1.10×10^{-7}	8.30×10^{-10}
$\epsilon = 1/2048$	5.48×10^{-4}	9.53×10^{-6}	1.10×10^{-7}	8.31×10^{-10}

Table 2
The l^2 errors of Bloch decomposition for the initial data (4.2).

M	6	8	10	12
$\epsilon = 1/128$	3.83×10^{-3}	1.15×10^{-4}	1.94×10^{-6}	2.07×10^{-8}
$\epsilon = 1/512$	3.83×10^{-3}	1.15×10^{-4}	1.94×10^{-6}	2.07×10^{-8}
$\epsilon = 1/2048$	3.83×10^{-3}	1.15×10^{-4}	1.94×10^{-6}	2.07×10^{-8}

Table 3
The l^2 errors of wave function for Example 2.

ϵ	1/128	1/512	1/2048
$\|\Phi^{\epsilon}_{GB} - \Psi^{\epsilon}\|_2$	6.41×10^{-2}	2.17×10^{-2}	9.92×10^{-3}

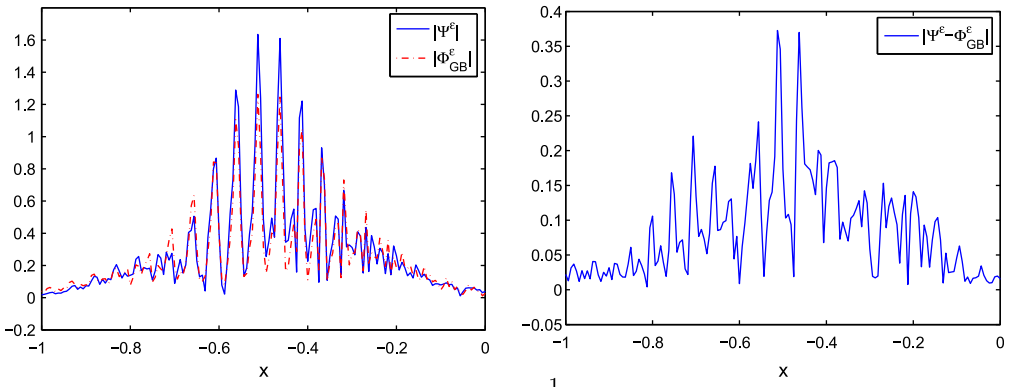

(a) $\varepsilon = \dfrac{1}{128}$

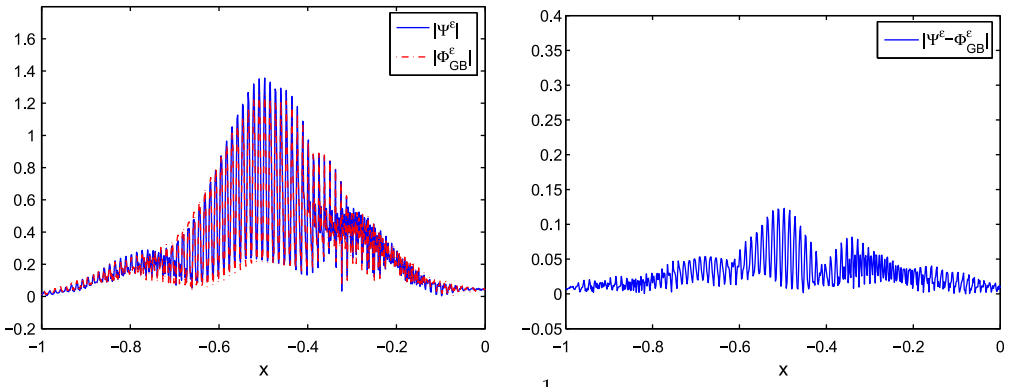

(b) $\varepsilon = \dfrac{1}{512}$

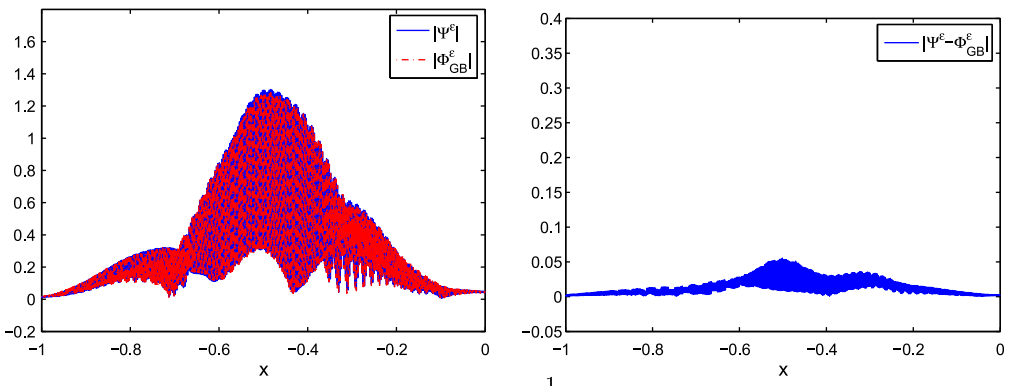

(c) $\varepsilon = \dfrac{1}{2048}$

Fig. 3. Example 2, the Schrödinger solution $|\Psi^\epsilon|$ versus the Gaussian beams solution $|\Phi^\epsilon_{GB}|$ at $\epsilon = \frac{1}{128}, \frac{1}{512}, \frac{1}{2048}$. The left figures are the comparisons of the wave amplitude at $t = 0.2$; the right figures plot the errors $|\Psi^\epsilon - \Phi^\epsilon_{GB}|$.

Table 4
The l^2 errors of wave function for Example 3.

ϵ	1/128	1/512	1/2048
$\|\Phi^\epsilon_{GB} - \Psi^\epsilon\|_2$	4.85×10^{-2}	1.43×10^{-2}	6.86×10^{-3}

4. Numerical examples

In this section, we test the accuracy of the Bloch decomposition-based Gaussian beam method by several numerical examples. The 'true' solution of the Schrödinger equation with periodic potentials is solved by the Strang splitting spectral method

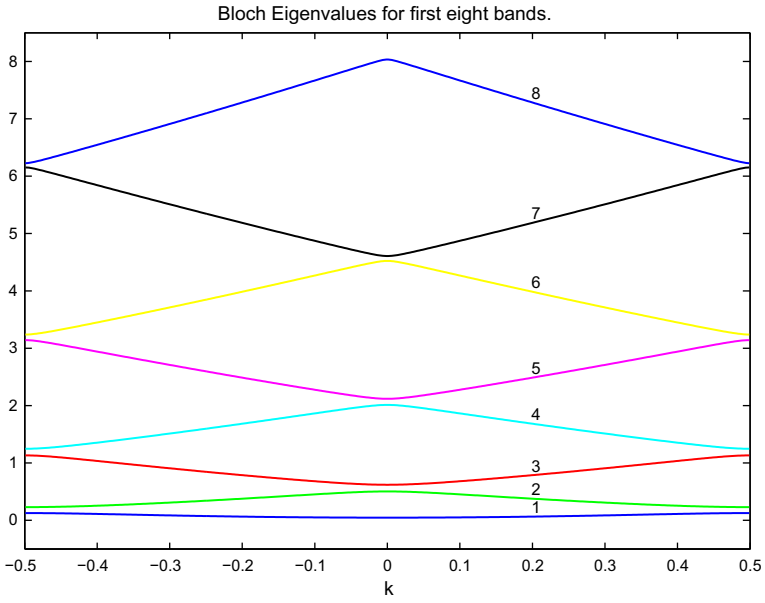

Fig. 5. The eigenvalues $E_m(k)$, $m = 1, \ldots, 8$ of the insulator example with $V_I(z) = e^{-20(z-\pi)^2}$.

which may numerically cause band crossing. The issue of band crossing is itself an interesting topic which will not be studied in this paper. To avoid unnecessary numerical complication, we do not put mesh points around the singular points ($k = 0, \pm 0.5$).

Example 1. We test the accuracy of the Bloch decomposition by the following two initial conditions

$$(1) \quad A_0(x,z) = e^{-50(x+0.5)^2}, \quad S_0(x) = 0.3x + 0.1\sin x, x \in [-1,0], \tag{4.1}$$

$$(2) \quad A_0(x,z) = e^{-50(x+0.5)^2}\cos z, \quad S_0(x) = 0.3x + 0.1\sin x, x \in [-1,0]. \tag{4.2}$$

The l^2 errors of the Bloch decomposition with different ϵ are given in Tables 1 and 2. As one can see, the errors are basically independent of ϵ and the accuracy is good even for small number of bands.

4.2. The Gaussian beam approximations

In this subsection, we conduct numerical experiments to show the efficiency and accuracy of the Bloch decomposition-based Gaussian beam method. We take the external potential $U(x) = 0$ for all the examples. This is not necessary for the numerical method, but is convenient for us to stay away from the singularity points of the Bloch eigenfunctions ($k = 0, \pm 0.5$). The solutions of the Liouville Eqs. (3.17)–(3.19) can be obtained using the method of characteristics:

$$\begin{aligned}
&\phi_m(t,y,\xi) = -i(y - E'_m(\xi)t) + \xi - S'_0(y - E'_m(\xi)t),\\
&S_m(t,y,\xi) = S_0(y - E'_m(\xi)t) + E'_m(\xi)\xi t - E_m(\xi)t,\\
&a_m(t,y,\xi) = \frac{a^0_m(y)}{\sqrt{1 + (i + S''_0(y - E'_m(\xi)t))E''_m(\xi)t}}.
\end{aligned}$$

We will denote the Eulerian Gaussian beam solution given by (3.23) as Φ^ϵ_{GB}. The grids are taken as $\Delta y = \Delta\xi = 1/N_y$ where N_y will be specified in each example.

Example 2. In this example, we take (4.1) as the initial data for the Schrödinger Eq. (1.1). The l^2 errors between the solution of the Schrödinger equation Ψ^ϵ and that of the Gaussian beam method Φ^ϵ_{GB} are given in Table 3. Here we take time $t = 0.2$, the number of Bloch bands $M = 8$, the number of Gaussian beams $N_y = 32$ (which is enough for numerical accuracy and shows the efficiency for small values of ϵ). The convergence rate in ϵ is of order 0.6730 in the l^2 norm. We plot the wave amplitudes and absolute errors for different ϵ in Fig. 3.

Example 3. In this example, the same experiments are carried out for initial data (4.2). With the same numerical parameters as in Example 2, the l^2 errors between the solution of the Schrödinger equation Ψ^ϵ and that of the Gaussian beam method Φ^ϵ_{GB} are given in Table 4. The convergence rate in ϵ is of order 0.7054 in the l^2 norm. We plot the wave amplitudes and absolute errors for different ϵ in Fig. 4.

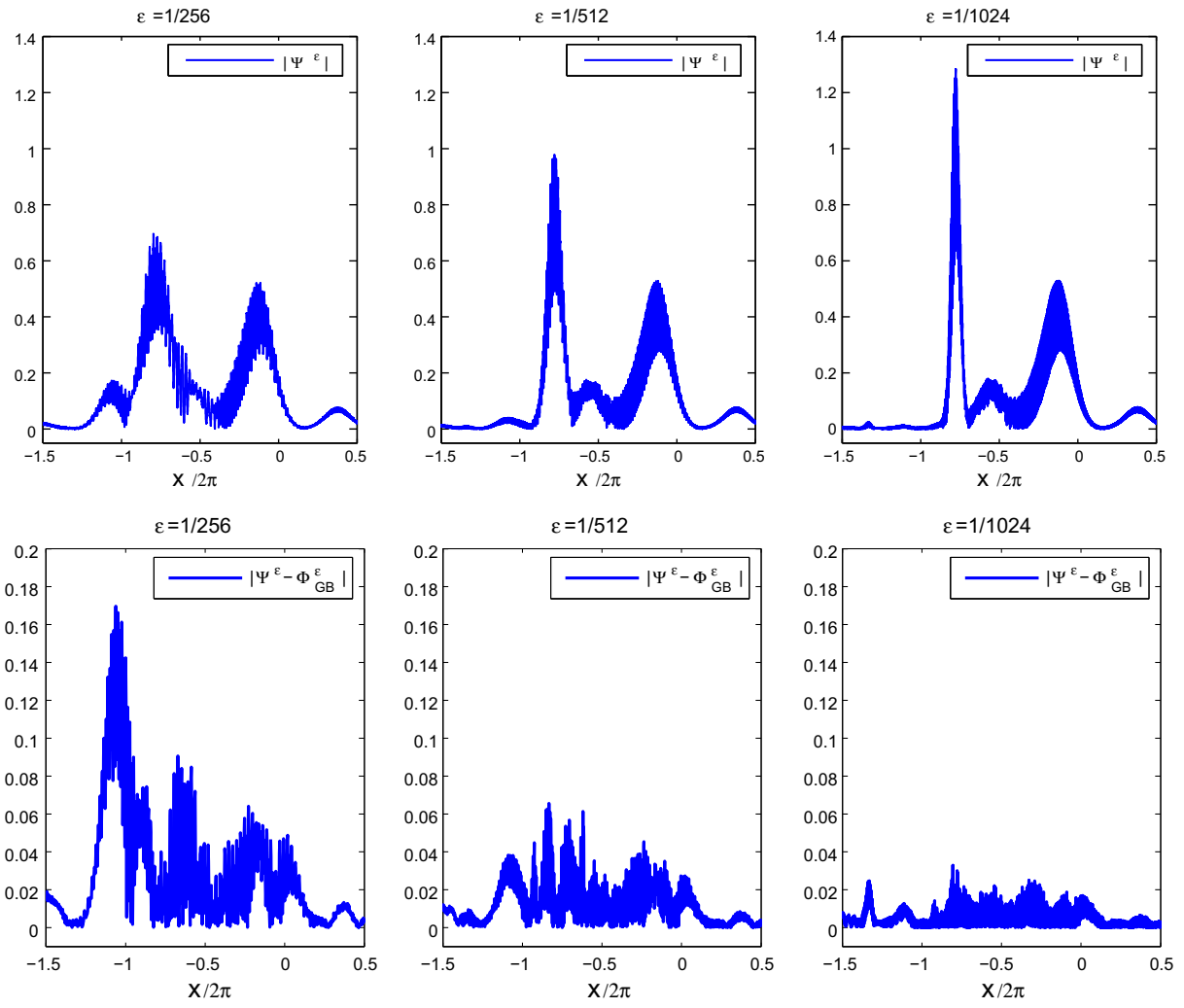

Fig. 6. Example 4, at time $t = 0.5$. Top: The wave amplitude for the 'exact' solution Ψ^ϵ with different ϵ. Bottom: The errors between the 'exact' solution Ψ^ϵ and the Gaussian beam solution Φ^ϵ_{GB}.

Table 5
The l^2 errors of wave function for Example 4.

(ϵ, N_y)	$(1/128.24)$	$(1/256.32)$	$(1/512.48)$	$(1/1024.64)$
$\|\Phi^\epsilon_{GB} - \Psi^\epsilon\|_2$	8.34×10^{-2}	4.27×10^{-2}	1.71×10^{-2}	7.25×10^{-3}

4.3. An application in the insulators

In this subsection, we study an insulator example where $V_\Gamma(z) = e^{-20(z-\pi)^2}$ [8]. This gives a band structure shown in Fig. 5. Since it is an insulator, the band gap is of $O(1)$ and does not allow the band crossing phenomenon to occur.

We use the semi-Lagrangian method introduced in [26] to compute $\psi^{\epsilon,m}_{eu}$. We take (3.17) for instance to illustrate the main idea. In order to get ϕ_m at the mesh point (y^j, ξ^k) (or the points needed around caustic points), one traces (y^j, ξ^k) back to the initial position (y^j_0, ξ^k_0) by solving (3.3) and (3.4) with $t \to -t$ numerically, which are the time-backward bi-characteristics of (3.17). Then one simply has $\phi_m(t, y^j, \xi^k) = \phi_m(0, y^j_0, \xi^k_0)$. (3.18) and (3.19) are treated similarly by changing $L_m \to d/dt$ and solving them along the time-backward bi-characteristics. We comment that one can still, for example, use the finite difference method to solve the Liouville Eqs. (3.17)–(3.19), but since we use the improved semi-Lagrangian method in Remark 3.1 to take care of the beam summation (3.23) around caustics, it will be more natural and convenient to also use this method to compute (3.17)–(3.19). The grids are taken as $\Delta y = \Delta\xi = 1/N_y$ and $\Delta t = \sqrt{\epsilon}/45$ where N_y will be specified in each case of ϵ.

Example 4. We consider the external harmonic potential $U(x) = \frac{1}{2}x^2$ and the initial conditions

$$A_0(x,z) = e^{-50(x+\pi)^2}\cos z, \quad S_0(x) = 0.3 - 0.3\sin x. \tag{4.3}$$

In this example, one caustic forms at time $t = 0.5$ which corresponding to the peaks around $x = -0.75$ in Fig. 6. We choose $[-3\pi, \pi]$ as the computational domain which is large enough so that the zero boundary condition could be applied. We take the number of Bloch bands $M = 8$ and the number of Gaussian beams $N_y \sim \epsilon^{-\frac{1}{2}}$ as discussed in [23]. The l^2 errors between the 'exact' solution Ψ^ϵ and the Gaussian beam solution Φ^ϵ_{GB} are given in Table 5, and plotted in Fig. 6. The convergence rate in ϵ is of order 1.17 in the l^2 norm.

5. Conclusion

In this paper, we developed an efficient Eulerian computational method for the linear Schrödinger equation with periodic potentials. Using the Bloch decomposition, we generalize the Gaussian beam method introduced in [23] to solve the problem with periodic potentials asymptotically with an error of $O(\sqrt{\epsilon})$, where ϵ is the small semiclassical parameter. While the classical numerical method, such as the recently developed Bloch decomposition based time-splitting spectral method, for the original Schrödinger equation requires the mesh size to be of $O(\epsilon)$, this new method requires the mesh size to be merely of $O(\sqrt{\epsilon})$. Several numerical examples are given to demonstrate the accuracy and effectiveness of this Bloch decomposition-based Gaussian beam method.

Acknowledgement

The authors would like to thank Prof. Weinan E for suggesting the insulator example used in Section 4.3. This work was partially supported by NSF Grant No. DMS-0608720, NSF FRG Grant DMS-0757285, NSAF Projects 10676017, NSFC Projects 10971115, the National Basic Research Program of China under Grant 2005CB321701. SJ was also supported by a Van Vleck Distinguished Research Prize from University of Wisconsin-Madison.

Appendix A

In this appendix, we give the detailed derivation of the Lagrangian formulation for the Bloch decomposition-based Gaussian beam method.

For convenience we drop the index m and denote the modified WKB ansatz as

$$\Psi^\epsilon(t,x,y) = a(t,y)\tilde{\chi}\Big(T_x, \frac{x}{\epsilon}\Big)e^{iT/\epsilon}, \tag{A.1}$$

where $y = y(t,y_0)$, $\tilde{\chi}(T_x, z := \frac{x}{\epsilon})$ is $\chi(k, z := \frac{x}{\epsilon})$ with the *real*-valued k replaced by the *complex*-valued T_x and $T = T(t,x,y)$ is given by

$$T(t,x,y) = S(t,y) + p(t,y)(x-y) + \frac{1}{2}M(t,y)(x-y)^2. \tag{A.2}$$

Note that when $x = y, T_x = p(t,y) \in \mathbb{R}$, which implies $\tilde{\chi}(T_x,z) = \chi(T_x,z)$. The properties of the eigenfunction $\tilde{\chi}(k,z)$ for *complex* k could be found in an early work of Kohn [25].

Since in the two-scale expansion $\mathrm{d}_x \to \partial_x + \frac{1}{\epsilon}\partial_z$, one has

$$\begin{aligned}
\Psi^\epsilon_t &= \left(\frac{\mathrm{d}a}{\mathrm{d}t}\tilde{\chi} + a\tilde{\chi}_k\frac{\mathrm{d}T_x}{\mathrm{d}t} + \frac{i}{\epsilon}a\tilde{\chi}\frac{\mathrm{d}T}{\mathrm{d}t}\right)e^{iT/\epsilon}\\
\mathrm{d}_x\Psi^\epsilon &= \left(a\tilde{\chi}_k T_{xx} + \frac{1}{\epsilon}a\tilde{\chi}_z + \frac{i}{\epsilon}a\tilde{\chi}T_x\right)e^{iT/\epsilon},\\
\mathrm{d}_x^2\Psi^\epsilon &= \left(a\tilde{\chi}_{kk}T_{xx}^2 + \frac{2}{\epsilon}a\tilde{\chi}_{kz}T_{xx} + a\tilde{\chi}_k T_{xxx} + \frac{2i}{\epsilon}a\tilde{\chi}_k T_{xx}T_x\right)e^{iT/\epsilon} + \left(\frac{1}{\epsilon^2}a\tilde{\chi}_{zz} + \frac{2i}{\epsilon^2}a\tilde{\chi}_z T_x - \frac{1}{\epsilon^2}a\tilde{\chi}T_x^2 + \frac{i}{\epsilon}a\tilde{\chi}T_{xx}\right)e^{iT/\epsilon}.
\end{aligned}$$

Plugging them into (1.1) and matching the leading order asymptotic coefficient give

$$(T_t + y_t T_y)\tilde{\chi} - \frac{1}{2}\tilde{\chi}_{zz} - iT_x\tilde{\chi}_z + \frac{1}{2}T_x^2\tilde{\chi} + V_\Gamma\tilde{\chi} + U\tilde{\chi} = 0,$$

which can be written as

$$[T_t + y_t T_y + U(x)]\tilde{\chi} = \frac{1}{2}(\partial_z + iT_x)^2\tilde{\chi} - V_\Gamma(z)\tilde{\chi}. \tag{A.3}$$

Evaluating (A.3) at $x = y$ gives

$$[S_t + y_t(S_y - p) + U(y)]\chi = \frac{1}{2}(\partial_z + ip)^2\chi - V_\Gamma(z)\chi,$$

where we have used the fact that when $x = y, T_x = p(t,y) \in \mathbb{R}$, which implies $\tilde{\chi}(T_x,z) = \chi(T_x,z)$. This fact will be used again later.

Making use of the Bloch eigenvalue problem (2.1)–(2.3), one has

$$[S_t + y_t(S_y - p) + U(y)]\chi = -H(p,z)\chi = -E(p)\chi,$$

which is equivalent to

$$S_t + y_t S_y - p y_t + E(p) + U(y) = 0. \tag{A.4}$$

Taking derivative with respect to x of (A.3) gives

$$(T_{xt} + y_t T_{xy} + U_x)\tilde{\chi} + (T_t + y_t T_y + U)\tilde{\chi}_k T_{xx} = iT_{xx}(\partial_z + iT_x)\tilde{\chi} + \left(\frac{1}{2}(\partial_z + iT_x)^2 - V_\Gamma(z)\right)\tilde{\chi}_k T_{xx}. \tag{A.5}$$

Evaluating (A.5) at $x = y$ yields

$$(p_t + y_t(p_y - M) + U_y)\chi + (S_t + y_t(S_y - p) + U)M\chi_k = iM(\partial_z + ip)\chi + \left(\frac{1}{2}(\partial_z + ip)^2 - V_\Gamma(z)\right)M\chi_k.$$

After simplification and taking inner product with χ of the above equation,

$$p_t + y_t p_y + U_y = [y_t - p + i\langle\chi_z, \chi\rangle]M + \langle(E - H)\chi_k, \chi\rangle M. \tag{A.6}$$

We introduce a theorem below which helps our further derivation.

Theorem A.1. *The derivatives of the Bloch eigenfunction $E(k)$ satisfy the following relations*

$$E'(k) = k - iu_3,$$
$$E''(k) = 1 + 2iu_2 + 2iu_1u_3,$$

where

$$u_1(k) = \langle\chi_k, \chi\rangle,$$
$$u_2(k) = \langle\chi_k, \chi_z\rangle = -\langle\chi_{kz}, \chi\rangle,$$
$$u_3(k) = \langle\chi_z, \chi\rangle.$$

Moreover, we have the equalities

$$\langle(E - H)\chi_k, \chi\rangle = 0,$$
$$\langle(E - H)\chi_{kk}, \chi\rangle = 0,$$
$$u_2 + \overline{u_2} + 2u_1u_3 = 0.$$

Proof. By taking derivatives of (2.2) with respect to k, we have

$$H_k\chi + H\chi_k = E\prime\chi + E\chi_k.$$

Taking inner product with χ, one gets

$$E' = \langle H_k\chi, \chi\rangle + \langle(H - E)\chi_k, \chi\rangle$$

The first term of the right-hand side above gives $k - iu_3$ because

$$H_k = -i\partial_z + k,$$

and the second term is zero since H is self-adjoint,

$$\langle(H - E)\chi_k, \chi\rangle = \langle\chi_k, (H - E)\chi\rangle = 0.$$

Hence we have

$$E'(k) = k - iu_3.$$

The other equalities could be easily proved similarly. □

Using these equalities, (A.6) becomes

$$p_t + y_t p_y + U_y = (y_t - E'(p))M. \tag{A.7}$$

Taking derivative with respect to x of (A.5), we have

$$(T_{xxt} + y_t T_{xxy} + U_{xx})\tilde{\chi} + 2(T_{xt} + y_t T_{xy} + U_x)\tilde{\chi}_k T_{xx} + (T_t + y_t T_y + U)\left(\tilde{\chi}_{kk}T_{xx}^2 + \tilde{\chi}_k T_{xxx}\right)$$
$$= iT_{xxx}(\partial_z + iT_x)\tilde{\chi} - T_{xx}^2\tilde{\chi} + 2iT_{xx}(\partial_z + iT_x)\tilde{\chi}_k T_{xx} + \left(\frac{1}{2}(\partial_z + iT_x)^2 - V_\Gamma(z)\right)\left(\tilde{\chi}_{kk}T_{xx}^2 + \tilde{\chi}_k T_{xxx}\right).$$

Evaluating the last equation at $x = y$ produces

$$(M_t + y_t M_y + U_{yy})\chi + 2(y_t - E\prime(p))\chi_k M^2 = (2y_t\chi_k - \chi + 2i\chi_{kz} - 2p\chi_k)M^2 + (E - H)\chi_{kk}M^2.$$

Taking inner product with χ and simplifying it lead to

$$(M_t + y_t M_y + U_{yy}) + 2(y_t - E\prime(p))M^2 u_1 = (2y_t u_1 - 1 - 2iu_2 - 2pu_1)M^2. \tag{A.8}$$

By matching the next order in the asymptotic expansion, one has,

$$(a_t + y_t a_y)\tilde{\chi} + a\tilde{\chi}_k(T_{xt} + y_t T_{xy}) - ia\tilde{\chi}_{kz}T_{xx} + a\tilde{\chi}_k T_{xx}T_x + \frac{1}{2}a\tilde{\chi}T_{xx} = 0.$$

Evaluating it at $x = y$ gives

$$(a_t + y_t a_y)\chi - a\chi_k U_y + a\chi_k(y_t - E'(p))M + \left(-\chi_k y_t - i\chi_{kz} + \chi_k p + \frac{1}{2}\right)aM = 0.$$

By taking the inner product with χ and simplifying it, one has

$$(a_t + y_t a_y) - au_1 U_y + au_1(y_t - E'(p))M + \left(-u_1 y_t + iu_2 + u_1 p + \frac{1}{2}\right)aM = 0. \tag{A.9}$$

Considering the y-trajectory defined by

$$\frac{dy}{dt} = E'(p),$$

and using the equalities

$$2y_t u_1 - 1 - 2iu_2 - 2pu_1 = 2E'u_1 - 1 - 2iu_2 - 2pu_1 = 2u_1(E' - p) - 1 - 2iu_2 = -2u_1 u_3 - 1 - 2iu_2 = -E'',$$

(A.4), (A.7)–(A.9) can be written as a set of ODEs:

$$\frac{dy}{dt} = E'(p), \tag{A.10}$$

$$\frac{dp}{dt} = -U_y, \tag{A.11}$$

$$\frac{dS}{dt} = pE'(p) - E(p) - U, \tag{A.12}$$

$$\frac{dM}{dt} = -E''M^2 - U_{yy}, \tag{A.13}$$

$$\frac{da}{dt} = au_1 U_y - \frac{1}{2}E''aM. \tag{A.14}$$

References

[1] N.W. Ashcroft, N.D. Mermin, Solid State Physics, Saunders, New York, 1976.
[2] G. Bal, A. Fannjiang, G. Papanicolaou, L. Ryzhik, Radiative transport in a periodic structure, J. Statist. Phys. 95 (1–2) (1999) 479–494.
[3] W. Bao, S. Jin, P.A. Markowich, On time-splitting spectral approximations for the Schrödinger equation in the semiclassical regime, J. Comput. Phys. 175 (2) (2002) 487–524.
[4] A. Bensoussan, J.L. Lions, G. Papanicolaou, Asymptotic analysis for periodic structures, Studies in Mathematics and its Applications, vol. 5, North-Holland Publishing Co., Amsterdam, New York, 1978.
[5] R. Carles, P.A. Markowich, C. Sparber, Semiclassical asymptotics for weakly nonlinear Bloch waves, J. Stat. Phys. 117 (1–2) (2004) 343–375.
[6] L.T. Cheng, H.L. Liu, S. Osher, Computational high frequency wave propagation using the level set method, with applications to the semi-classical limit of Schrödinger equations, Commun. Math. Sci. 1 (2003) 593–621.
[7] M. Dimassi, J.C. Guillot, J. Ralston, Gaussian beam construction for adiabatic pertubations, Math. Phys. Anal. Geom. 9 (3) (2006) 187–201.
[8] C. Garcia-Cervera, J.F. Lu, Y. Xuan, W. E, A linear scaling subspace iteration algorithm with optimally localized non-orthogonal wave functions for Kohn-Sham density functional theory, preprint.
[9] L. Gosse, Using K-branch entropy solutions for multivalued geometric optics computations, J. Comput. Phys. 180 (1) (2002) 155–182.
[10] L. Gosse, Multiphase semiclassical approximation of an electron in a one-dimensional crystalline lattice II. Impurities, confinement and Bloch oscillations, J. Comput. Phys. 201 (2004) 344–375.
[11] L. Gosse, The numerical spectrum of a one-dimensional Schrödinger operator with two competing periodic potentials, Commun. Math. Sci. 5 (2007) 485–493.
[12] L. Gosse, P.A. Markowich, Multiphase semiclassical approximation of an electron in a one-dimensional crystalline lattice-I. Homogeneous problems, J. Comput. Phys. 197 (2004) 387–417.
[13] L. Gosse, N. Mauser, Multiphase semiclassical approximation of an electron in a one-dimensional crystalline lattice III. From ab initio models to WKB for Schrödinger-Poisson, J. Comput. Phys. 211 (2006) 326–346.
[14] G.A. Hagedorn, Semiclassical quantum mechanics. I. The $h \to 0$ limit for coherent states, Commun. Math. Phys. 71 (1980) 77–93.
[15] E.J. Heller, Cellular dynamics: a new semiclassical approach to time-dependent quantum mechanics, J. Chem. Phys. 94 (1991) 2723–2729.
[16] E.J. Heller, Guided Gaussian wave packets, Acc. Chem. Res. 39 (2006) 127–134.
[17] N.R. Hill, Gaussian beam migration, Geophysics 55 (11) (1990) 1416–1428.
[18] Z. Huang, S. Jin, P.A. Markowich, C. Sparber, A Bloch decomposition-based split-step pseudospectral method for quantum dynamics with periodic potentials, SIAM J. Sci. Comput. 29 (2) (2007) 515–538.

[19] Z. Huang, S. Jin, P.A. Markowich, C. Sparber, Numerical simulation of the nonlinear Schrodinger equation with multi-dimensional periodic potentials, SIAM Multiscale Model. Simul. 7 (2008) 539–564.
[20] Z. Huang, S. Jin, P.A. Markowich, C. Sparber, On the Bloch decomposition-based spectral method for wave propagation in periodic media, Wave Motion 46 (2009) 15–28.
[21] S. Jin, H. Liu, S. Osher, R. Tsai, Computing multivalued physical observables the semiclassical limit of the Schrödinger equations, J. Compun. Phys. 205 (2005) 222–241.
[22] S. Jin, S. Osher, A level set method for the computation of multivalued solutions to quasi-linear hyperbolic PDEs and Hamilton–Jacobi equations, Commun. Math. Sci. 1 (3) (2003) 575–591.
[23] S. Jin, H. Wu, X. Yang, Gaussian beam methods for the Schrodinger equation in the semi-classical regime: Lagrangian and Eulerian formulations, Commun. Math. Sci. 6 (4) (2008) 995–1020.
[24] S. Jin, X. Yang, Computation of the semiclassical limit of the Schrödinger equation with phase shift by a level set method, J. Sci. Comput. 35 (2-3) (2008) 144–169.
[25] W. Kohn, Analytic properties of Bloch waves and Wannier functions, Phys. Rev. 115 (1959) 809–821.
[26] S. Leung, J. Qian, R. Burridge, Eulerian Gaussian beams for high frequency wave propagation, Geophysics 72 (2007) 61–76.
[27] H. Liu, Z. Wang, A Bloch band based level set method for computing the semiclassical limit of Schrödinger equations, J. Comput. Phys. 228 (9) (2009) 3326–3344.
[28] C. Min, Simplicial isosurfacing in arbitrary dimension and codimension, J. Comput. Phys. 190 (1) (2003) 295–310.
[29] M. Motamed, O. Runborg, Taylor expansion errors in Gaussian beam summation, preprint.
[30] M. Motamed, O. Runborg, A wave front-based Gaussian beam method for computing high frequency waves, preprint.
[31] S. Osher, L.-T. Cheng, M. Kang, H. Shim, Y.-H. Tsai, Geometric optics in a phase-space-based level set and Eulerian framework, J. Comput. Phys. 179 (2) (2002) 622–648.
[32] G. Panati, H. Spohn, S. Teufel, Motions of electrons in adiabatically perturbed periodic structures, Analysis, modeling and simulation of multiscale problems, 595–617, Springer, Berlin, 2006.
[33] D. Peng, B. Merriman, S. Osher, H. Zhao, M. Kang, A PDE based fast local level set method, J. Comput. Phys. 155 (1999) 410–438.
[34] M.M. Popov, A new method of computation of wave fields using Gaussian beams, Wave Motion 4 (1982) 85–97.
[35] J. Ralston, Gaussian beams and the propagation of singularities, Studies in PDEs, MAA Stud. Math. 23 (1982) 206–248.
[36] G. Sundaram, Qian Niu, Wave-packet dynamics in slowly perturbed crystals: Gradient corrections and Berry-phase effects, Phys. Rev. B 59 (1999) 14915–14925.
[37] N.M. Tanushev, Superpositions and higher order Gaussian beams, Commun. Math. Sci. 6 (2) (2008) 449–475.
[38] N.M. Tanushev, J.L. Qian, J. Ralston, Mountain waves and Gaussian beams, SIAM Multiscale Model. Simul. 6 (2007) 688–709.
[39] X. Wen, High order numerical methods to two dimensional delta function integrals in level set methods, preprint.
[40] C.H. Wilcox, Theory of Bloch waves, J. Anal. Math. 33 (1978) 146–167.